More about orbitally excited hadrons from lattice QCD

Thomas A. DeGrand and Matthew W. Hecht*
Department of Physics, University of Colorado, Boulder, Colorado 80309
(Received 8 June 1992)

This is the second of two papers describing the calculation of spectroscopy for orbitally excited states from lattice simulations of quantum chromodynamics. New features include higher statistics for P-wave systems and first results for the spectroscopy of D-wave mesons and baryons, for relatively heavy-quark masses. We parametrize the Coulomb gauge wave functions for P- and D-wave systems and compare them to those of their corresponding S-wave states.

PACS number(s): 12.38.Gc, 11.15.Ha, 14.20.−c, 14.40.−n

I. INTRODUCTION

Recently, we presented some preliminary results from an exploratory calculation of the masses of P-wave mesons and baryons from lattice Monte Carlo simulations of quantum chromodynamics in a quenched approximation with Wilson fermions [1]. This paper describes the final results from these simulations. We have increased the statistics of our P-wave study. There is a hint of some fine-structure splitting in the charmonium system. We also present first results for a D-wave spectroscopy of fairly heavy-quark mesons and baryons. Finally, we show some of the properties of Coulomb-gauge meson and baryon wave functions of P- and D-wave systems and compare them to S-wave wave functions at the same quark masses [2].

Only recently has lattice QCD spectroscopy begun to move beyond ground-state hadrons. Some P-wave-state masses are regularly measured in staggered simulations because they are the odd-parity partners of "ordinary" states: The a_1 and ρ are examples of such pairs. In nonrelativistic QCD, Thacker and Lepage [3] have computed the masses of χ_C and χ_B states (without including spin effects). Few Wilson simulations have been conducted to study P-wave states. The APE Collaboration [4] measured masses of some P-wave mesons in quenched simulations at $6/g^2=\beta=5.7$, but has had difficulty in continuing their program to higher β [5]. Recently, El-Khadra *et al.* have presented a calculation of the $1P$-$1S$ splitting in charmonium, which they use to fix the strong-coupling constant [6]. This calculation was done with a smaller lattice spacing than the one we report here and with an improved action for the fermions.

Calculations of the masses of orbital excitations in lattice simulations are difficult for three reasons: First, one needs to measure a correlation function with nonzero overlap onto the desired L sector and zero overlap on $L=0$; otherwise, the signal will be dominated at large t, by the lighter $L=0$ states. Our methodology solves this problem. Second, the signal is intrinsically noisy [7]. A diagonal correlator $C(t)=\langle 0|\Gamma(t)\Gamma(0)|0\rangle$, which falls off at large t like $\exp(-E_1 t)$, where E_1 is the energy of the lightest state which the operator Γ can create from the vacuum, has fluctuations given by

$$\sigma_\Gamma^2=\frac{1}{N}[\langle|\Gamma(t)\Gamma(0)|^2\rangle-C(t)^2]\ . \tag{1.1}$$

Because of its first term, σ_Γ^2 decays with a mass of the lightest particle $|\Gamma|^2$ can make from the vacuum. If Γ is a meson operator (creating a $\bar{q}q$ pair), Γ^2 will create a $q^2\bar{q}^2$ state, which will most likely couple to a $\pi\pi$ pair. Its correlator will fall like $\exp(-2m_\pi t)$. In the baryon sector, $|\Gamma|^2$ will make a $q^3\bar{q}^3$ state, and the lightest such state is three pions. Thus we expect a signal-to-noise ratio to be a falling function of t: $\sigma/C_H(t)\simeq\exp(m_H-m_\pi)t$ for mesons and $\sigma/C_H(t)\simeq\exp(m_H-3/2m_\pi)t$ for baryons. This is a more serious problem for orbitally excited states than for S-wave states because their energy differences are larger. Finally, the baryon sector includes multiple states with the same quantum numbers, which will appear in the same correlators. For example, in the $L=1$ [70] of SU (6) [8], the nonstrange sector includes one $j=\frac{5}{2}$ and two $j=\frac{3}{2}$ and $\frac{1}{2}$ nucleons and $j=\frac{3}{2}$ and $\frac{1}{2}$ Δ's.

II. METHODOLOGY

A. Construction of orbitally excited states

We construct orbitally excited states by using interpolating fields which couple only to a specific angular momentum eigenstate, which are projected onto zero momentum and which are of large spatial extent to maximize overlap with the state. Our strategy is to look at correlators of different operators at $t=0$ and $t\neq 0$.

At the $t\neq 0$ end of the correlation function, we use an operator which depends on the relative separation of the quarks, which is conventionally referred to as a "wave function" [9]. The wave function $\psi_G(r)$ of a hadron H in a guage G is defined as

$$\psi_G(r)=\sum_{\mathbf{x}}\langle H|q(\mathbf{x})\bar{q}(\mathbf{x}+\mathbf{r})|0\rangle\ , \tag{2.1}$$

where $q(\mathbf{x})$ and $\bar{q}(\mathbf{y})$ are quantum-mechanical operators which create a quark and an antiquark at locations $\mathbf{x}$ and $\mathbf{y}$. (We have suppressed Dirac and color indices.) Our correlation function is constructed from convolutions of quark and antiquark propagators $G(x,y)$:

*Present address: National Center for Atmospheric Research, P.O. Box 3000, Boulder, CO 80307.

$$C(\mathbf{r},t)=\sum_{\mathbf{x}}\langle 0|\Psi(\mathbf{y}_1,\mathbf{y}_2)G_q(\mathbf{y}_1,0;\mathbf{x},t)\times G_{\bar{q}}(\mathbf{y}_2,0;\mathbf{x}+\mathbf{r},t)|0\rangle\ , \tag{2.2}$$

where $\Psi(\mathbf{y}_1,\mathbf{y}_2)$ is the $t=0$ operator. At large t, if the mass of the hadron is m_H, then

$$C(\mathbf{r},t)\simeq\exp(-m_H t)\psi_G(\mathbf{r})\ , \tag{2.3}$$

and so by plotting $C(\mathbf{r},t)$ as a function of $\mathbf{r}$ we can reconstruct the wave function up to an overall constant. We measure the mass of a state by convoluting $C(\mathbf{r},t)$ with some test function which further projects out the desired state:

$$C(t)=\sum_{\mathbf{r}}\psi^*_{\text{test}}(\mathbf{r})C(\mathbf{r},t)\ . \tag{2.4}$$

At $t=0$ we take an operator which is separable in the coordinates of the quarks. For a meson we use

$$\Psi(x_1,x_2)=\phi_1(x_1)\phi_2(x_2)\ . \tag{2.5}$$

In order to couple to orbital excitations, we take ϕ_1 to be an S wave and ϕ_2 to be some orbitally excited state with angular momentum l, centered around some specified coordinate. This state is a linear superposition of a $\mathbf{p}=0$, $L=l$ orbital excitation and a state whose center-of-mass momentum is nonzero (this is the familiar "translation mode" of a shell-model state). Convoluting quark propagators as in Eq. (2.2) removes the $\mathbf{p}\neq 0$ state and gives us the wave function of the $\mathbf{p}=0$, $L=l$ state.

B. Spin considerations

We did not construct a complete set of P- or D-wave mesons and baryons. Instead, we proceeded as follows (for P waves): We worked in a basis in which γ_0 is diagonal. Our sources and sinks were chosen to couple only to the upper (large) components of the Dirac spinor. We constructed propagators for S-wave quarks with $m_S=\pm\frac{1}{2}$ and for P-wave quarks with $m_l=1$, $m_S=\pm\frac{1}{2}$. We can then completely construct the $|jm\rangle=|22\rangle$ $^3P_2$ and $|jm\rangle=|11\rangle$ $^1P_1$ mesons, as well as the $|jm\rangle=|\frac{5}{2}\,\frac{5}{2}\rangle$ nucleon $N(\frac{5}{2})$. We formed two other meson states with $S=1$ and $m_j=1$ and 0 ($m_S=0$ and -1), which are not angular momentum eigenstates; while we will label them as $^3P_1$ and $^3P_0$, they couple to all three ^3P states. [The "$^3P_1$" state is $(\uparrow\downarrow+\downarrow\uparrow)|11\rangle$; the "$^3P_0$" state is $(\downarrow\downarrow)|11\rangle$.] If the ordering of states on the lattice were as in charmonium, the lightest state in the channel would have the smallest j for a given m_j and the wave functions would in fact project out the states which they label. In the baryon sector, we constructed uud bound states with $m_j=\frac{3}{2}(\uparrow\uparrow\downarrow)|11\rangle$ and $-\frac{1}{2}(\downarrow\downarrow\downarrow)|11\rangle$.

D-wave spectroscopy is identical apart from the substitution of $l=2$ for $l=1$: We completely construct the $^3D_3$ and $^1D_2$ meson states and construct $m_j=2$ and 1 states which overlap $^3D_2$ and $^3D_1$ states. We construct nucleons of $m_j=\frac{7}{2}$, $\frac{3}{2}$, and $\frac{1}{2}$.

This is an incomplete construction forced on us by computer-memory limitations and a desire to keep the calculation simple. A dedicated simulation should do this properly, but will need many more quark propagators. Note also that while we are using nonrelativistic wave functions, they have the quantum numbers appropriate to the desired states and will couple to them, and not to S-wave states, regardless of whether the quarks are actually relativistic.

C. Details of the simulations

We performed the simulations using the Connection Machine CM-2 at the Pittsburgh Supercomputing Center. Our data set consists of 80 lattices for P-wave studies, of which the last 50 were also analyzed for D-wave systems, computed in quenched approximation at coupling $\beta=6$, separated by a combination of microcanonical overrelaxed [10] and Kennedy-Pendleton quasi-heat-bath [11] sweeps (100 passes of a pattern of 4 overrelaxed sweeps through the lattice and 1 heat-bath sweep). The lattice size is 16^4 sites. We gauge-fixed each of the lattice configurations to Coulomb gauge using an overrelaxation algorithm [12]. We used Wilson fermions. We used a fast matrix inverter provided by Liu of Thinking Machines, Inc. [13] to construct quark propagators. We computed P-wave spectroscopy at three hopping parameters corresponding to relatively heavy-quark masses, $\kappa=0.130$, 0.1450, and 0.1520, and D-wave spectroscopy at $\kappa=0.1300$ and 0.1450. The pseudoscalar mass in lattice units at these three κ's is 1.43, 0.83, and 0.56. We used heavy quarks because the size of the wave function for the orbitally excited states is much larger than the size of an S-wave bound state, and if the quark mass becomes too small, the wave function is squeezed by the simulation volume.

In Eq. (2.4) we use a test function $\psi_{\text{test}}=\exp[-(r/r_0)^2]r^l Y_l^l(\Omega)$, in the relative coordinate. We take ϕ_1 in Eq. (2.5) to be a Gaussian centered at the origin and ϕ_2 to be $\exp[-(r/r_0)^2]r^1 Y_l^l(\Omega)$. [As a technical note, when the width of the Gaussian becomes large compared with the size of the lattice, one must worry about edge effects. We do that by replacing the spherical harmonic by a function which has the same symmetry but is periodic in the box (of size L): $Y_1^1=(x+iy)/r\rightarrow(\sin 2\pi x/L+i\sin 2\pi y/L)/r$.] The width of the Gaussians used in Ψ and ψ_{test} was taken to be 2, 2, and $2\sqrt{2}$ lattice spacings for the three κ's.

We recorded wave functions for $^3P_2$, $^1P_1$, $^3D_3$, and $^1D_2$ mesons and for $N(\frac{5}{2})$ and $N(\frac{7}{2})$ baryons, at time slices 4, 5, and 6. All baryon wave functions pin the two quarks in a relative S state to the same coordinate. We folded meson data onto one octant of the spatial lattice and baryon data onto one quadrant before storing it and, in addition, kept data on one plane without folding.

III. WAVE FUNCTIONS

A. Pictures of wave functions

We now display some of the features of P- and D-wave functions and compare some of their simple observables with those of S-wave mesons of our earlier study [2]. We begin our display of results for wave functions by show-

ing some pictures of Coulomb-gauge meson and baryon wave functions.

In Figs. 1 and 2, we display plots of the real part of the wave function in the plane $z=0$ for a $\kappa=0.152$ $N(\frac{5}{2})$ baryon and a $\kappa=0.145$ $^3D_3$ meson, respectively. The contours show the locations where ψ is a multiple of 20% of its maximum value. The data for these graphs have not been spatially averaged. They show the characteristic dipole and quadrupole structure of the appropriate spherical harmonic. The fact that these distributions are not symmetric gives the reader an impression of the fluctuations in the data. They also give some idea of the extent to which the granularity of the lattice distorts the state and the extent to which the state fits into the simulation volume.

In order to illustrate further the extent to which a state fits in the simulation volume, we display in Fig. 3 a set of three-dimensional contours of constant absolute value of the real part of the wave function. This figure, for the $\kappa=0.145$ $^3D_3$ meson, shows the characteristic four-lobe quadrupole structure whose outer regions are compromised by the simulation volume. This is a problem for all the lighter-mass states; all the $\kappa=0.130$ mesons appear to fit reasonably well into the simulation volume.

Finally, we extract the radial wave function $f(r)$ itself from

$$f(r)=\mathrm{Re}\psi(\mathbf{r})/\mathrm{Re}Y_l^l(\Omega)\ . \tag{3.1}$$

The Coulomb-gauge radial wave functions for $\kappa=0.145$ $^3P_2$ and $^3D_3$ mesons are shown in Figs. 4 and 5. They appear to show the characteristic linear and quadratic zeros of the wave function at the origin.

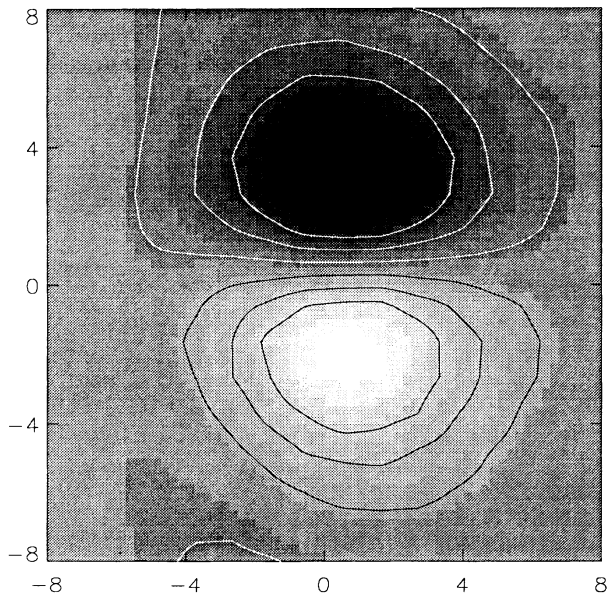

FIG. 1. Wave function of the $\kappa=0.152$ $N(\frac{5}{2})$ baryon in the plane $z=0$. The contours show interpolated lines of constant real ψ in multiples of 0.2 times the maximum value of ψ. The shading shows the value of the wave function (black is the most negative, white the most positive), interpolating from the original 16^2 lattice to a 64^2 grid.

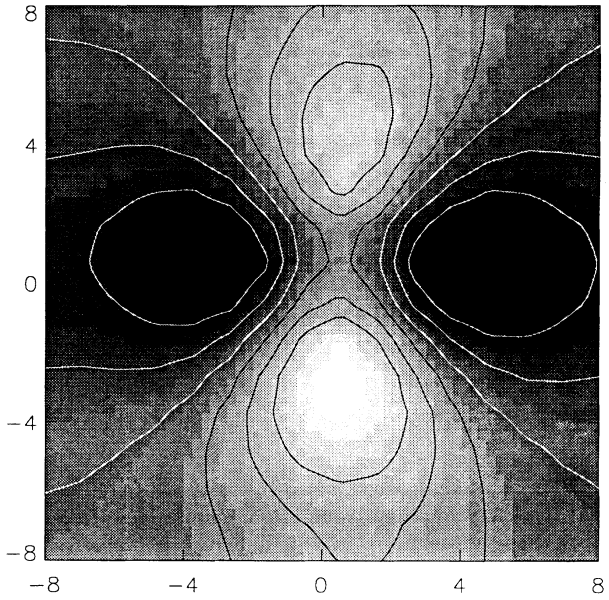

FIG. 2. Wave function of the $\kappa=0.145$ $^3D_3$ meson in the plane $z=0$. The contours and shading are parametrized as in Fig. 1.

B. Fitting wave-function parameters

The goal of this section is to provide simple analytical parametrizations of wave functions which can be used for future studies of spectroscopy and to provide checks for calculations of wave-function properties performed directly on the data.

Fitting the wave functions proved to be unexpectedly difficult because of the high correlations among wave functions at different separations. With only 50 or 80 lattices, we had to fit a subset of the data, since correlated

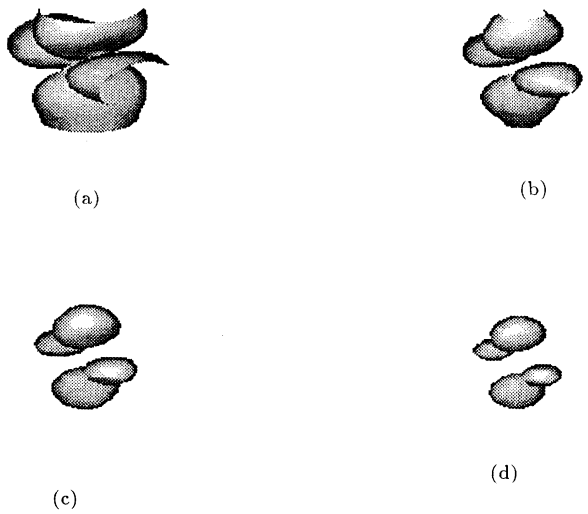

FIG. 3. Surfaces of constant absolute amplitude of the $\kappa=0.145$ $^3D_3$ meson in three dimensions, in fractions of its maximum: (a) $|\psi|=0.2\psi_{\max}$, (b) $|\psi|=0.4\psi_{\max}$, (c) $|\psi|=0.5\psi_{\max}$, and (d) $|\psi|=0.6\psi_{\max}$. The "breaks" in the surfaces in (a) and (b) occur when the surfaces intersect the edge of the simulation volume.

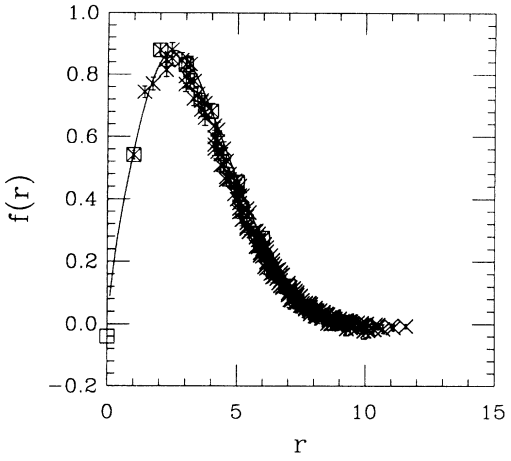

FIG. 4. Radial wave function of the $\kappa=0.145$ $^3P_2$ meson. Crosses show all points; squares are points along the x axis used to fit the wave function (fit is the line).

fits require more lattices than fitted points. We elected to choose coordinates along axes where the spherical harmonic was unity (up to a sign); this gives us seven ($z=1-7$) points to fit. We folded all directions related by reflections onto this axis with the necessary signs. Then we fit the radial wave function $f(r)$, including a periodic or antiperiodic image term from the boundary [we fit $f_{\rm test}(r)=g(r)\pm g(L-r)$].

After a certain amount of trial and error, we chose to fit to

$$g(r)=A(r+br^2)\exp(-cr)\ , \tag{3.2}$$

for P waves, and

$$g(r)=A(r^2+br^4)\exp(-cr)\ , \tag{3.3}$$

for D waves, plus image terms, and we believe that many other simple functional forms would work as well. The data cannot distinguish between these or more complicated functions, and if we try to force a fit, the Hessian matrix becomes singular. We fit the baryon data to the same parameters (recall that we have pinned two quarks together, and so there is only one relative coordinate left).

The data are very correlated, and the matrix of correlations very singular. It was not unusual to find correlation matrices whose conditioning number (ratio of largest to smallest eigenvalue) approached several thousand. The conditioning number was not stable: Fitting half the lattices in a data set could cause the conditioning number to vary by a factor of 2. We would also achieve a considerable variation in the conditioning number by varying elements in the correlation matrix by hand by a percent or so. In contrast, the correlation matrices for propagators had conditioning numbers on the order of 50 and were quite stable under the same tests. Typically, in a 7×7 correlation matrix, only the largest 3 or 4 eigenvalues remained reasonably stable as the number of lattices in the data set was varied. Therefore we adopted the following strategy for determing the parameters in $f(r)$: We looked at uncorrelated fits, correlated fits to all parameters (very unstable), correlated fits in which the correlation matrix had its smallest three eigenvalues removed (via singular value decomposition), and correlated fits to a subset of the data (often $r=1,3,5,7$). In the latter case, one could not use consecutive points, since either one or both of the correlation matrix or Hessian matrix would become singular. The D-wave data was much more difficult to deal with with than the P-wave data in this respect.

The overall normalization of the wave function is not important for spectroscopy studies. The parameters b and c for P-wave mesons are displayed in Fig. 6 and for D-wave mesons in Fig. 7.

C. Moments of wave functions

The nth moment of the meson wave function is defined in terms of $\psi(\mathbf{r})$ as

$$\langle r^n\rangle=\frac{\int r^2dr(r/2)^n f(r)^2}{\int r^2dr\, f(r)^2}\ . \tag{3.4}$$

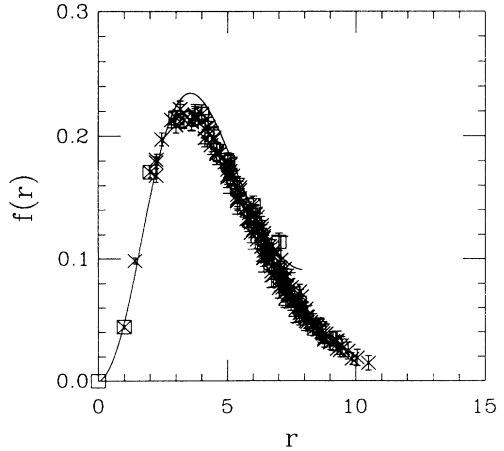

FIG. 5. Radial wave function of the $\kappa=0.145$ $^3D_3$ meson. Crosses show all points; squares are points used to fit the wave function (fit is the line).

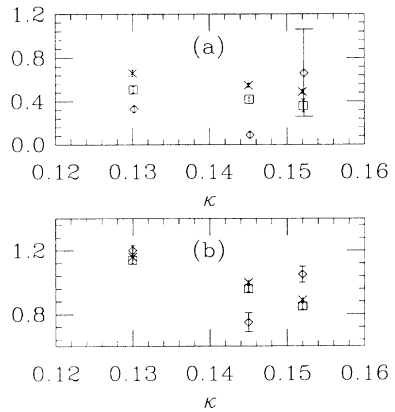

FIG. 6. Fit parameters of P-wave wave functions: (a) b parameter and (b) c parameter. Points are labeled with crosses for $^3P_2$ mesons, squares for $^1P_1$ mesons, and diamonds for $N(\frac{5}{2})$ baryons.

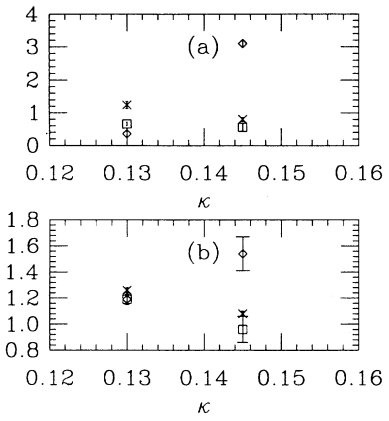

FIG. 7. Fit parameters of D-wave wave functions: (a) b parameter and (b) c parameter. Points are labeled with crosses for ${}^3D_3$ mesons, squares for ${}^1D_2$ mesons, and diamonds for $N(\frac{7}{2})$ baryons.

The factor of $\frac{1}{2}$ is included so that the second moment defined this way (when appropriately weighted by quark charges) reduces to the second moment of the quark-charge distribution defined through the form factor.

We determined the first and second moments of our meson wave functions in two ways: First, we computed it directly from the data, by performing a single-elimination jacknife analysis, and second, we computed it using the fitted form of wave functions. We consider the second method to be more reliable since in many cases the wave function is still large at the edge of the simulation volume. Only a fit which includes image effects can correctly reproduce the tail of the wave function.

In all cases and for both jacknife and using the fitted radial wave function, the values of the two moments were independent of time slice, although the uncertainty increases with increasing t. We display the first and second moments at $t=4$ in Figs. 8 and 9, respectively. We see that, while the two methods give rather similar results for

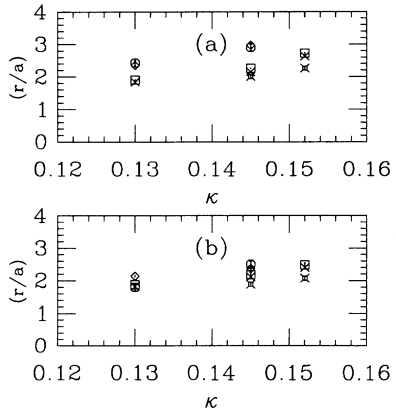

FIG. 8. First moment of P- and D-wave meson wave functions (a) from a jackknife analysis and (b) from the fitted radial wave functions. Points are labeled with crosses for ${}^3P_2$, squares for ${}^1P_1$, diamonds for ${}^3D_3$, octagons for ${}^1D_2$ mesons, and fancy squares for the pseudoscalar (data from Ref. [2]).

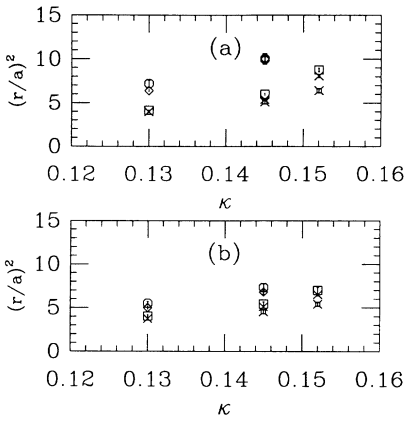

FIG. 9. Second moment of P- and D-wave meson wave functions (a) from a jackknife analysis and (b) from the fitted radial wave functions. Points are labeled as in Fig. 8.

the $\kappa=0.1300$ mesons, at smaller quark mass the discrepancy becomes pronounced.

The P-wave functions are larger than the S-wave wave functions, and the D-wave ones are larger still. Note that the diameter of the wave function in the simulation is 4 times $\langle r \rangle$ of Eq. (3.4), so that the simulation volume we use would appear to be too small for D-wave systems made of ligher quarks.

IV. SPECTROSCOPY

We extracted masses from our data by fitting the correlation function $C(t)$ of Eq. (5) in the standard way and looked at "effective masses' [local slope of $C(t)$] and fits to a range $t_{\min}$ to $t_{\max}=n_t/2=8$. All data are fit including the effects of correlations at different times [14].

As a general rule for selecting the best-fit value to present in a figure or table, we use "fit histograms." A fit is represented by a rectangle centered on the best-fit value for a mass μ, with a width given by (twice) the uncertainty of the fit (i.e., $\mu\pm\Delta\mu$) and a height which is the confidence level of the fit (to emphasize good fits) times the number of degrees of freedom (to emphasize fits over big distance ranges) divided by the statistical error on the parameter (to emphasize fits with small errors). The fit with the greatest height is the one we quote. This was the method used to select the best mass in an earlier S-wave spectroscopy calculation [15].

A. P-wave spectroscopy

Figure 10 shows effective masses and fits to a range of t values for the meson and baryon data.

All baryon masses at all κ values appear to be consistent; there is little sign of a drift of the masses with choice of fitting range. There is no evidence of any fine-structure splitting in any of the κ values. One cannot say whether this is due to a small intrinsic splitting on the lattice or whether all operators are merely coupling strongly to the $j=\frac{5}{2}$ nucleon. In our extrapolations, we will make the latter assumption.

The $\kappa=0.1300$ mesons also have stable, consistent fits.

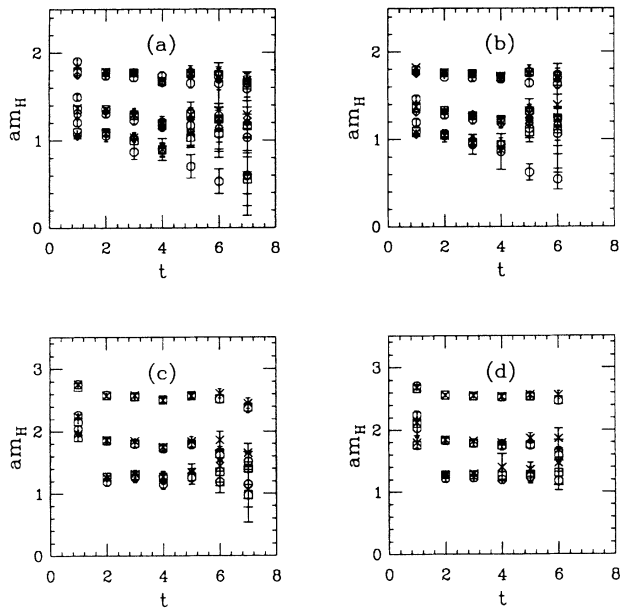

FIG. 10. Spectroscopy of P-wave mesons and baryons: (a) meson effective masses, (b) meson fits to a range, (c) baryon effective masses, and (d) baryon fits to a range. The three bands (in order of increasing mass) correspond to $\kappa=0.152$, 0.145, and 0.130. In each meson group, the $^1P_1$ state is labeled by a cross, the $^3P_0$ state by an octagon, the $^3P_1$ state by a square, and the $^3P_2$ state by a diamond. For baryons, the cross labels the $P_{1/2}$ state, the octagon the $P_{3/2}$ state, and the square the $P_{5/2}$ state.

The best-fit values from histograms all begin at $t=2$. There is a hint of the appearance of fine-structure splitting in the multiplet, as shown in Fig. 11. The splitting qualitatively resembles charmonium fine-structure splitting, with the $^3P_0$ state the lightest and the other states more nearly degenerate. However, uncertainties are so large that this probably should not be taken too seriously. These data seem to be limited by statistics.

The $\kappa=0.1450$ data is noisier by about a factor of 2. The $^3P_2$ state is heavier than the $^1P_1$. The $^3P_0$ signal never stabilizes; while the fit from $t_{\min}=2$ is satisfactory

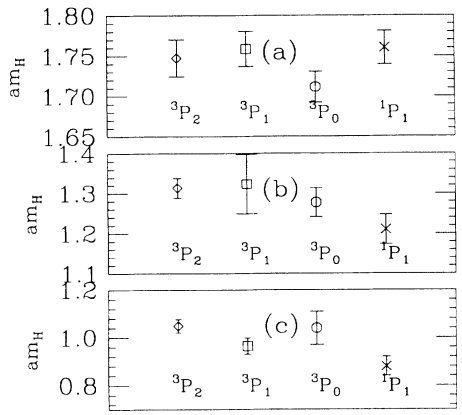

FIG. 11. Fine-structure splitting in the P-wave meson multiplets: (a) $\kappa=0.130$, (b) $\kappa=0.145$, and (c) $\kappa=0.152$.

from the point of view of χ^2 (7.0 for 5 degrees of freedom), fits at increasing $t_{\min}$'s produce monotonically falling masses. Fit histograms are shown in Fig. 12. The $^3P_1$ state is degenerate with the $^3P_2$, but with large errors.

Finally, the $\kappa=0.1520$ data share the same features as the $\kappa=0.1450$ data, with slightly larger uncertainties. The P-wave lattice masses are listed in Table I.

B. D-wave spectroscopy

The D-wave data is noisier than the P-wave data (as expected). Typical uncertainties for masses are about 0.08; 4 times the P-wave value. All masses appear to be asymptotic by $t_{\min}=2-3$, and all signals disappeared into the noise by $t=6$. Because the data are so noisy, we could see no evidence for fine-structure splitting in a multiplet. Figure 13 shows effective masses and fits to a range of t values for the meson and baryon data. The masses are listed in Table II.

C. Comparison with experiment

It is difficult to convert these lattice numbers into reliable quantities which can be compared with experiment. At $\beta=6.0$, one is far from the scaling region. S-wave spectroscopy with Wilson fermions does not agree with experiment. The quark hopping parameters we have used are very distant from the zero quark-mass value. We will glance at two comparisons, but we have to say that with the quality of the signals they should probably not be taken very seriously as other than qualitative observations.

The masses are shown in Fig. 14. First, if we extrapolate all masses linearly in κ to $\kappa_c=0.1567$, we find $am(^3P_2)=0.93(3)$, $am(^1P_1)=0.73(4)$, and $am(N(\frac{5}{2}))=1.07(4)$, and the D-wave meson and baryon

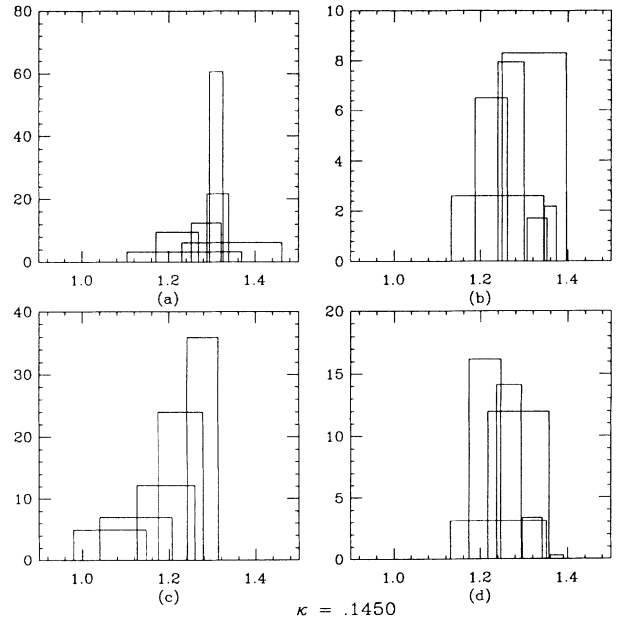

FIG. 12. "Fit histograms" of $\kappa=0.145$ P-wave mesons: (a) $^3P_2$ mesons, (b) $^3P_1$ mesons, (c) $^3P_0$ mesons, and (d) $^1P_1$ mesons.

TABLE I. P-wave meson and baryon masses in lattice units.

κ	State	Mass
0.1300	$^3P_2$	1.747(23)
0.1300	$^3P_1$	1.759(22)
0.1300	$^3P_0$	1.712(19)
0.1300	$^1P_1$	1.760(21)
0.1450	$^3P_2$	1.313(25)
0.1450	$^3P_1$	1.322(74)
0.1450	$^3P_0$	1.278(35)
0.1450	$^1P_1$	1.210(37)
0.1520	$^3P_2$	1.05(3)
0.1520	$^3P_1$	0.96(3)
0.1520	$^3P_0$	1.03(7)
0.1520	$^1P_1$	0.88(4)
0.1300	baryon	2.56(2)
0.1450	baryon	1.79(4)
0.1520	baryon	1.28(4)

are at 1.18(10) and 1.93(20), respectively. The proton mass at κ_c from our S-wave wave-function study [2] is $am(N)=0.55(1)$, and so we have $m(^3P_2)/m(N)=1.70(6)$, $m(^1P_1)/m(N)=1.33(8)$, and $m(N(\frac{5}{2}))/m(N)=1.94(8)$, and the ratios of the D-wave meson and baryon to the nucleon mass are 2.14(18) and 3.5(4), respectively.

Experimental data corresponding to these states are $m(a_2)/m(N)=1.40$ or $m(f_2)/m(N)=1.35$, $m(b1)/m(N)=1.31$, $m(N(1675))/m(N)=1.78$, $m(\rho_3(1690))/m(N)=1.80$, and $m(N(2220))/m(N)=2.36$. The P-

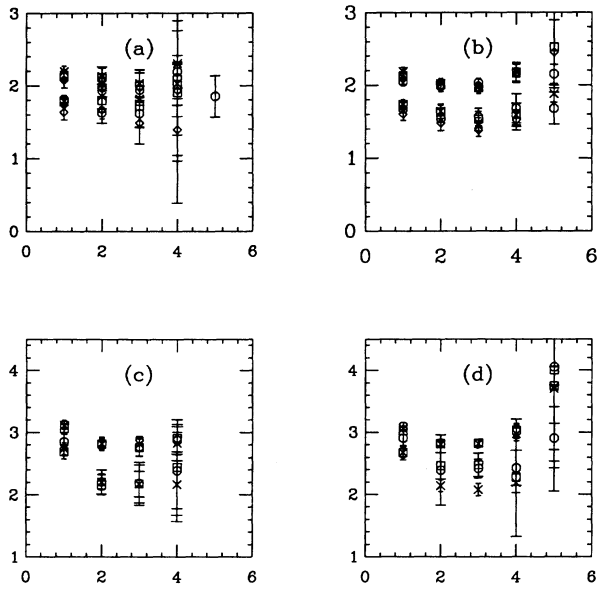

FIG. 13. Spectroscopy of D-wave mesons and baryons: (a) meson effective masses, (b) meson fits to a range, (c) baryon effective masses, and (d) baryon fits to a range. The two bands (in order of increasing mass) correspond to $\kappa=0.145$ and 0.130. In each meson group, the $^1D_2$ state is labeled by a cross, the $^3D_1$ state by an octagon, the $^3D_2$ state by a square, and the $^3D_3$ state by a diamond. For baryons, the cross labels the $D_{1/2}$ state, by octagon the $D_{5/2}$ state, and the square the $D_{7/2}$ state.

TABLE II. D-wave meson and baryon masses in lattice units.

κ	State	Mass
0.1300	meson	2.00(6)
0.1450	meson	1.54(5)
0.1300	baryon	3.0(1)
0.1450	baryon	2.4(1)

wave masses look qualitatively correct, but the D-wave states (from which the extrapolation in κ is enormous) are too high.

As another comparison with experiment, we can try to predict the mass of the D-wave states in charmonium. To do this, we must extrapolate in κ from our $\kappa=0.1300$ data point to the charm mass. We also need a value for the lattice spacing a, which could vary by 30% at this β value, depending on how it is chosen. We determine κ and a by taking lattice determinations of the $^3P_2$ and $^3S_1$ states at $\kappa=0.130$, 0.145, and 0.152 and extrapolating their masses linearly in κ. (We use the data of Ref. [16] for the $\kappa=0.1300$ vector meson.) We determine the lattice spacing by fitting the extrapolated masses to the $\psi(3095)$ and $\chi(3555)$ masses. This gives a charm hopping parameter of $\kappa=0.1224$ and an inverse lattice spacing of $1/a=1790$ MeV. (Note that determining the lattice spacing from our proton-mass data would give $1/a=1710$ MeV; from the ρ meson, $1/a=2264$ MeV.) The extrapolated common D-meson mass is then 3.99(16) MeV, where the error is only from the extrapolation. The $^3D_1$ $c\bar{c}$ state is at 3.77 GeV, but its mass is influenced by the nearby $D\bar{D}$ threshold. Model calculations [17] of D-wave states (some of which are narrow since their decays to $D\bar{D}$ are forbidden) give masses of 3.81–3.84 GeV. At this value of the lattice spacing, our $^3P_2$-$^3P_0$ mass splitting at $\kappa=0.1300$ is 63 MeV; in charmonium, the corresponding number is 145 MeV.

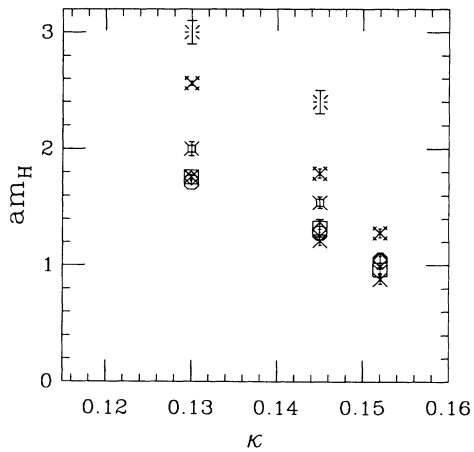

FIG. 14. Masses of P- and D-wave hadrons as a function of hopping parameter. Diamonds labels $^3P_2$ mesons, squares $^3P_1$, octagons $^3P_0$, and crosses $^1P_1$. P-wave baryons are labeled with a fancy cross, D-wave mesons with a fancy square, and D-wave baryons with a burst.

V. CONCLUSIONS

In retrospect, many aspects of the project could have been done better. We should have completely reconstructed the spin structure of all the different states. We should have recorded wave functions for all time slices and not just for big t's. Then we could have used the wave functions we determined in Sec. III as the input for $\psi_{\text{test}}(r)$ for spectroscopy calculations.

It is clear that this program could be carried to arbitrarily high angular momentum states. To do so will probably require very high statistics, a more fine-grained lattice (since the lobe structure of the angular part of the wave function becomes more pronounced), and a larger simulation volume, since the size of the wave function grows with angular momentum.

Note that the uncertainties on the P-wave masses fell by about a factor of 2 when the data set increased from 20 to 80 lattices. This suggests that the calculations of P-wave meson masses are almost certainly limited only by statistics. Meson P-wave spectroscopy still needs to improve its uncertainties by another factor of 2–4 before it can begin to make a serious comparison with experimental data, but we believe that this would be an easy thing for any large-scale spectroscopy simulation to do. A reliable method for identifying specific baryon states remains to be demonstrated.

ACKNOWLEDGMENTS

We would like to thank C. Liu for providing us with a copy of his matrix inverter. The computations described in this work were carried out at the Pittsburgh Supercomputing Center. The work was supported by the U.S. Department of Energy.

[1] T. DeGrand and M. Hecht, Phys. Lett. B **275**, 435 (1992).
[2] M. W. Hecht and T. DeGrand, Phys. Rev. D **46**, 2155 (1992).
[3] B. Thacker and G. P. Lepage, Phys. Rev. D **43**, 196 (1991).
[4] P. Bacilieri *et al.*, Phys. Lett. B **214**, 115 (1988); Nucl. Phys. **B317**, 509 (1989).
[5] S. Cabasino *et al.*, Phys. Lett. B **258**, 195 (1991).
[6] A. El-Khadra, G. Hockney, A. Kronfeld, and P. Mackenzie, Phys. Rev. Lett. **69**, 729 (1992); P. Mackenzie, in *Lattice '91,* Proceedings of the International Symposium on Lattice Field Theory, Tsukuba, Japan, 1991, edited by M. Fukugíta, Y. Iwasaki, M. Okawa, and A. Ukawa [Nucl. Phys. (Proc. Suppl.) **26**, 369 (1992)]; *ibid.*, p. 372.
[7] See G. P. Lepage, in *From Actions to Answers,* Proceedings of the 1989 Theoretical Advanced Summer Institute on Particle Physics, Boulder, Colorado, 1989, edited by T. DeGrand and D. Toussaint (World Scientific, Singapore, 1990).
[8] J. Kokkedee, *The Quark Model* (Benjamin, New York, 1969).
[9] Wave functions computed in a smooth gauge were first introduced by B. Velikson and D. Weingarten, Nucl. Phys. **B249**, 433 (1985), and by S. Gottlieb, in *Advances in Lattice Gauge Theory,* edited by D. Duke and J. Owens (World Scientific, Singapore, 1985). Other recent uses, for heavy-light-quark systems are described by E. Eichten, in *Lattice '90,* Proceedings of the International Symposium, Tallahassee, Florida, 1990, edited by U. Heller, A. Kennedy, and S. Sanielevici [Nucl. Phys. (Proc. Suppl.) **20**, 475 (1991)]; and C. Bernard, J. Labrenz, and A. Soni, *ibid.,* p. 488. A gauge-invariant formalism has been described by M.-C. Chu, M. Lassia, and J. W. Negele, Nucl. Phys. **B360**, 31 (1991).
[10] F. Brown and T. Woch, Phys. Rev. Lett. **58**, 2394 (1987); M. Creutz, Phys. Rev. D **36**, 55 (1987). For a review, see S. Adler, in *Lattice '88,* Proceedings of the International Symposium on Lattice Field Theory, Batavia, Illinois, 1988, edited by A. Kronfeld and P. Mackenzie [Nucl. Phys. B (Proc. Suppl.) **9**, 437 (1989)].
[11] A. Kennedy and B. Pendleton, Phys. Lett. **156B**, 393 (1985).
[12] J. E. Mandula and M. C. Ogilvie, Phys. Lett. B **248**, 156 (1990).
[13] C. Liu, in *Lattice '90* [9], p. 149.
[14] For a good introduction to error analysis, see D. Toussaint, in *From Actions to Answers* [7].
[15] K. Bitar *et al.*, Phys. Rev. Lett. **65**, 2106 (1990); Phys. Rev. D **42**, 3794 (1990).
[16] T. DeGrand and R. Loft, Phys. Rev. D **39**, 2678 (1989).
[17] Compare E. Eichten *et al.*, Phys. Rev. D **21**, 203 (1980) (3.81 GeV); W. Buchmüller and S.-H. Tye. *ibid.* **24**, 132 (1981) (3.81 GeV); W. Kwong, J. Rosner, and C. Quigg, Annu. Rev. Nucl. Part. Sci. **37**, 325 (1987), quote $m(^3D_2)=3.81$ GeV, $m(^3D_3)=3.84$ GeV, and $m(^1D_2)=3.82$ GeV from the model of P. Moxhay and J. Rosner, Phys. Rev. D **28**, 1132 (1983).

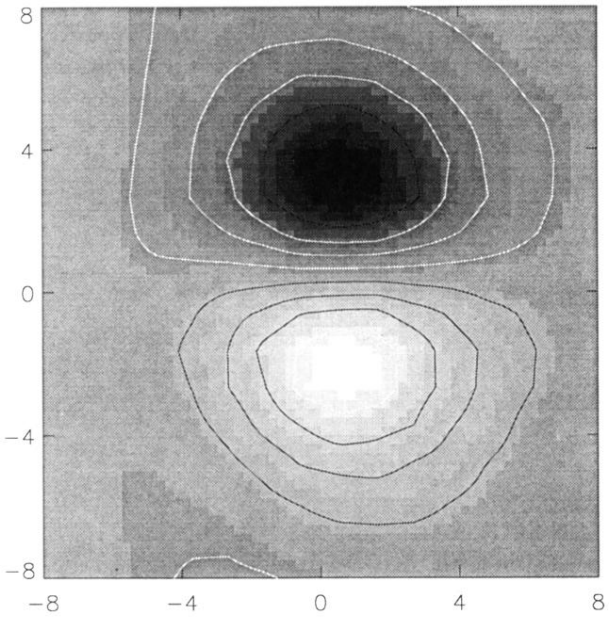

FIG. 1. Wave function of the $\kappa=0.152$ $N(\frac{5}{2})$ baryon in the plane $z=0$. The contours show interpolated lines of constant real ψ in multiples of 0.2 times the maximum value of ψ. The shading shows the value of the wave function (black is the most negative, white the most positive), interpolating from the original 16^2 lattice to a 64^2 grid.

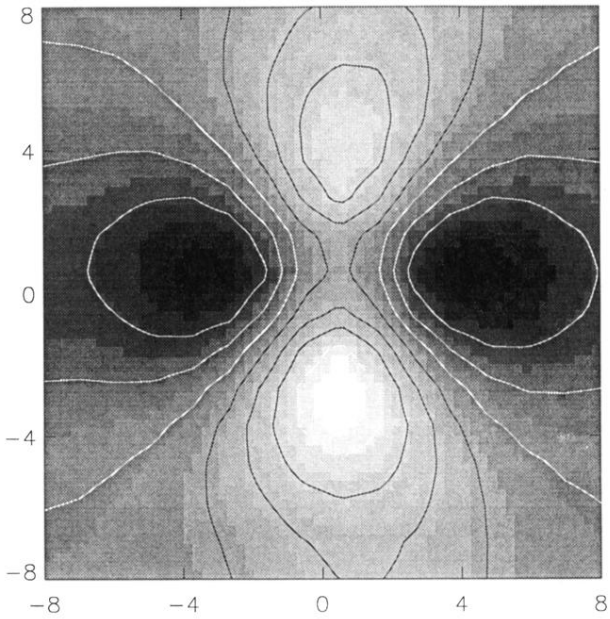

FIG. 2. Wave function of the $\kappa=0.145$ $^3D_3$ meson in the plane $z=0$. The contours and shading are parametrized as in Fig. 1.

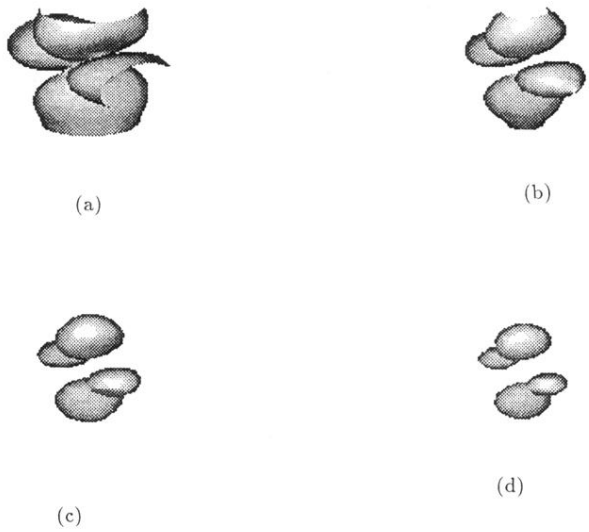

FIG. 3. Surfaces of constant absolute amplitude of the $\kappa=0.145$ $^3D_3$ meson in three dimensions, in fractions of its maximum: (a) $|\psi|=0.2\psi_{\max}$, (b) $|\psi|=0.4\psi_{\max}$, (c) $|\psi|=0.5\psi_{\max}$, and (d) $|\psi|=0.6\psi_{\max}$. The "breaks" in the surfaces in (a) and (b) occur when the surfaces intersect the edge of the simulation volume.